Masters Report

University of Toronto Department of Physics

August 21, 2008

A Study of Jet and Missing Transverse Energy Reconstruction and Data Cleaning Techniques on ATLAS Calorimeter Cosmic Ray Data

Travis Bain
995981834

Abstract

Monte Carlo generated QCD jets, and jets reconstructed from cosmic ray data are analyzed and compared. This comparison allows some of the first opportunities to run through a full study, from data collection, to reconstruction, to analysis, within ATLAS, using real events. The ability to handle data at every step of the way will be crucial in achieving a "steady-state" mode of operation in the coming months and years of ATLAS operation. The use of electromagnetic fractions as a data cleaning technique within the ATLAS calorimeter system is also studied and shown to be a robust tool in removing high energy cosmic ray events as a background from jet and E_T^{Miss} distributions.

I'd like to express my appreciation to the high energy faculty and students at University of Toronto and many others within the ATLAS Canada Collaboration. In Particular, many thanks to Richard Teuscher, Gabe Rosenbaum, and Adam Gibson.

Contents

1 Introduction

The Standard Model of particle physics is one of science's greatest achievements. It is capable of making theoretical predictions that accord, with great precision, to experimental results. Yet, despite all of its success, the collective theories are unsustainable under high energy conditions. Theorists have been exploring these situations for a number of years, and have made tremendous progress in numerous directions; however they continue to proceed without the guidance of experimental data. The goal of the Large Hadron Collider (LHC) is to explore the TeV energy scale and provide some guidance for theoretical predictions within, and beyond, the Standard Model.

The LHC is a circular proton-proton (pp) collider that will achieve a center of mass energy of 14 TeV and a luminosity of $10^{34}\ cm^{-2}\ sec^{-1}$ [1]. It has had one successful test of its beam transfer system on August 10, 2008, with another scheduled for August 22, 2008 leading to the first attempt of a full circulating beam on September 10, 2008 [2]. The LHC will host five independent experiments; the ATLAS experiment is one of two general purpose detectors which will focus on the discovery of new particles.

1.1 Nomenclature

In this study the beam direction defines the z-axis, and the x-y plane is the plane transverse to the beam direction. The positive x-axis is defined as pointing from the interaction point, in the center of ATLAS, to the center of the LHC ring, and the positive y-axis is pointing upward from the interaction point. The azimuthal angle ϕ is measured around the beam axis, and the polar angle, θ, is measured from the beam axis. The pseudorapidity is defined by $\eta = -\ln(\tan(\theta/2))$. The transverse momentum (P_T), transverse energy (E_T), and missing transverse energy (E_T^{Miss}) are all defined in the x-y plane. Seperations in pseudorapidity-azimuthal angle space are defined as $\Delta R = \sqrt{\Delta\eta^2 + \Delta\phi^2}$. Finally, side A of the detector is defined as the side with positive z, and side C is the side with negative z [1].

1.2 The ATLAS Detector

The ATLAS detector is most easily described as four separate systems: the inner detector, the muon spectrometer, the magnet systems,and the calorimeters. The inner detector is composed of three separate detectors, namely the pixel detector, the semiconductor tracker, and the transition radiation tracker. The purpose of the inner detector components is to track the position of charged particles away from the interaction point. The muon spectrometer focuses on detection of penetrating muons. The magnet system is composed of three separate systems: the central solenoid, the barrel toroid and the endcap toroid. The magnet fields produced by the magnetic system will bend the trajectories of charged particles, allowing their momenta to be measured by the inner detector and the muon spectrometer. Finally, the calorimeters measure the energy of particles, and will be the focus of this study.

The ATLAS Electromagnetic (EM) and Hadronic (HAD) calorimeters are located within the barrel, and endcap regions of the detector. The EM Calorimeter ($|\ \eta\ | < 3.2$) is a liquid-argon (LAr) sampling calorimeter which uses lead plates as the absorber to induce EM showers. The Hadronic Barrel Calorimeter (Tile) ($|\ \eta\ | < 1.7$) is a scintillator-tile calorimeter which uses

steel as an absorber and scintillating plastic, and photo-multiplier tubes, to detect hadronic showers. In both the Electromagnetic (EMEC) and Hadronic (HEC) End-Cap, LAr is used with lead for the EMEC and copper for the HEC. Finally the Forward Calorimeters (FCal) ($3.1 >| \eta |> 4.9$) also utilize LAr technology with the electromagnetic modules using copper, and the hadronic modules using tungsten; the FCal is uniquely positioned to play a crucial role in the identification of E_T^{Miss} and jet tagging [1].

1.3 Jets and Missing Transverse Energy in ATLAS

Jets and E_T^{Miss}, will play a central role in the ATLAS experiment once the LHC begins operation. A jet can be thought of as a well collimated grouping of stable particles produced by the hadronization of a quark or gluon following a hard scatter in a pp collision. Due to QCD confinement, color charged particles such as quarks and gluons cannot exist freely. Therefore when a quark or gluon is imparted with a large amount of energy from a hard scatter, the particle will fragment into numerous hadrons before it can be observed. For practical experimental purposes a jet can be described simply as a collection of particles contained in a well-defined region of $\eta - \phi$ space [3]. The ability to accurately reconstruct jets, from calorimeter signals, is crucial to nearly all physics to be done with the ATLAS detector. An absolute uncertainty of jet energy less than 1% is desirable to reconstruct the top quark mass, or reconstruct some supersymmetric final states [4].

E_T^{Miss} is an imbalance of energy in the transverse plane of the detector. One of the best known sources of E_T^{Miss} is neutrinos created via weak interactions which pass directly through the whole detector without interacting, however this is not considered further in this study. E_T^{Miss} is initially minimized in events that have no real E_T^{Miss}, by the nearly hermetic coverage of the calorimeter system in the pseudorapidity range $| \eta |< 4.9$ [4]. However, there still exist calorimeter imperfections, cracks, and dead, distorted or noisy cells that must be thoroughly understood in order to achieve accurate E_T^{Miss} distributions. Event topologies which include jets and E_T^{Miss} are extremely well suited to the study of many new physics channels, particularly supersymmetry and extra dimensions as their presence will be inferred through E_T^{Miss} [1].

1.4 Commissioning and Cosmic Rays

The commissioning of ATLAS, which has brought it from *installed* to *operational*, proceeds in four phases: 1) subsystem standalone commissioning, 2) integrating subsystem data acquisition (DAQ) with the overall ATLAS DAQ, 3) cosmic rays runs, and 4) single beam and first collisions [5]. This study focuses on the detection of cosmic rays, which provide the very first real data for ATLAS to analyze.

This cosmic ray commissioning has been carried out through ATLAS milestone weeks and weekend runs, which act as a rehearsal to get all the subsystems working together and the detector operating as one experiment. The data analyzed in this study came from a cosmic run taken during milestone week 7 (M7) in May 2008.

1.5 Analysis

The analysis in this study focuses on two main areas. The first is the comparison of Pythia generated JX jet events (see section 3.1) to reconstructed jets from cosmic ray data. Transverse momentum, E_T^{Miss}, and effective mass distributions are analyzed. The second is an examination of the electromagnetic fraction as a data cleaning technique to remove cosmic rays as a source of fake E_T^{Miss} from the QCD jet background. Again transverse momentum, E_T^{Miss}, and effective mass distributions are analyzed and the ATLANTIS Event Display is used to observe pulse shapes in the LAr calorimeters.

2 Jet and E_T^{Miss} Reconstruction Algorithms in ATLAS

The ATHENA framework, used within the ATLAS collaboration, is a control framework that provides the skeleton on which all event reconstruction and simulation is done [6]. Within ATHENA individual users are able to configure the official, packaged algorithms via services such as JobOptionSvc, which is a catalog of user-modifiable Algorithms, Tools and Services [7].

2.1 Jet Reconstruction

The ATLAS calorimeter system is the primary detector for measurement of jet properties [4]. Since the various calorimeters are composed of roughly 200,000 individual cells [8] of varying size and readout technologies, it is first necessary to combine these cells into larger objects with meaningful four-momenta. The two objects considered are *calorimeter towers* and *topological clusters* [4].

Calorimeter towers are formed by projecting the calorimeter cells onto a fixed grid in $\eta - \phi$ space. The tower size is $\Delta\eta \times \Delta\phi = 0.1 \times 0.1$ over the whole calorimetry region with 6,400 towers in total [4]. All the cells in the calorimeters calculate energy at the electromagnetic energy level, thus the tower signal is too at the electromagnetic energy scale, with no hadronic calibration taking place [4].

Topological cell clusters are the other object considered in jet reconstruction. Unlike the two-dimensional projection of towers, topological cell clustering is an attempt to reconstruct three-dimensional groups of energy representing the shower for each particle entering the calorimeter [4]. The clustering begins by finding a seed cell with a signal-to-noise ratio, $\Gamma = E_{cell}/\sigma_{noise,cell}$, above a certain threshold, $S = 4$. At this stage, all cells, in all three dimensions, neighboring the seed cells are added to the cluster. Neighbors of neighbor cells which have Γ above a secondary threshold, $N = 2$, are also added to the cluster. Finally, a ring of cells with Γ above a basic threshold, $P = 0$, are added to form the final cluster. Clusters, like towers are also measure energy at the electromagnetic energy scale, with no hadronic calibration taking place [4].

Once the basic objects have been formed the reconstruction of jets in ATLAS proceeds primarily via two different jet finding algorithms: seeded fixed-cone jet finders and sequential recombination jet finders [4]. Fixed-cone jet finders begin by ordering all input objects (towers or topological clusters) in order of decreasing transverse momentum (p_T), and setting what is called a "seed P_T threshold". If the object with the highest P_T is above the seed threshold, the next closest object within a cone in $\eta - \phi$ space with $\Delta R < R_{cone}$ (where R_{cone} is the fixed

cone radius) is combined with the seed and new direction for the cone is calculated from the combined four-momenta[1)] [4]. This process continues until the cone becomes stable, meaning the center of the cone is no longer shifting, at which point a new seed is searched for and the process begins for the second jet until no more seeds are available.

The sequential recombination jet finder in ATLAS is the k_t algorithm [4]. The k_t algorithm does not make use of seeds the way fixed cone finders do; instead all pairs of input objects ij are examined with respect to their relative transverse momentum squared,

$$d_{ij} = min(p_{Ti}^2, p_{Tj}^2)\frac{\Delta R_{ij}^2}{R^2} = min(p_{Ti}^2, p_{Tj}^2)\frac{\Delta\eta_{ij}^2+\Delta\phi_{ij}^2}{R^2},$$

and the squared p_T of object i relative to the beam $d_i = p_{Ti}^2$. If $d_{ij} < d_i$, objects i and j have their four-momenta combined, otherwise object i is considered to be a jet by itself. The free distance parameter, R, allows for control of the jet size[2)]. The algorithm is finished when all objects are a part of a jet, or a jet themselves [4].

This study will exclusively consider Cone 7 Tower Jets ($R = 0.7$). The reasons for this are two-fold. First, topological clusters require a great deal of understanding of the signal-to-noise ratio, something that is still very much under study at this time with regards to cosmic ray reconstruction. Second, once the LHC begins operation the first Analysis Object Data (AOD) produced will contain only Cone Tower Jets, as these are the easiest to understand, and there exists experience using these jets (ex. Tevatron) [9].

2.2 E_T^{Miss} Reconstruction

The reconstruction of E_T^{Miss} is accomplished primarily using transverse energy deposits in the calorimeters and muon tracks reconstructed using the muon spectrometer. There are two seperate algorithms used to reconstruct E_T^{Miss} in ATLAS: cell-based reconstruction and object based reconstruction [10].

The cell-based reconstruction algorithm utilizes three quantities to obtain a final E_T^{Miss} value. Namely contributions from the transverse energy deposites in the calorimeters, corrections for energy loss in the cryostats, and measured muons

$$E_T^{Miss,Final} = E_T^{Miss,Calo} + E_T^{Miss,Cryo} + E_T^{Miss,Muon}.$$

The $E_T^{Miss,Calo}$ term is calculated from the transverse energies measured in topological clusters:

$$E_{x,y}^{Miss,Calo} = -\sum_{TopoClust} E_{x,y}.$$

The total $E_T^{Miss,Calo}$ can then be obtained by adding the transverse energies in quadrature

$$E_T^{Miss,Calo} = -\sqrt{(E_x^{Miss,Calo})^2 + (E_y^{Miss,Calo})^2}.$$

[1)] The default configurations for ATLAS are a seed with $P_T > 1GeV$, and two cone sizes, $R_{cone} = 0.4$ and $R_{cone} = 0.7$

[2)] The default configurations for ATLAS are $R = 0.4$ for narrower jets and $R = 0.6$ for wider jets

The $E_T^{Miss,Muon}$ term is calculated from the momenta of muons measured in a large range of pseudorapidity ($|\eta| < 2.7$):

$$E_{x,y}^{Miss,Muon} = -\sum_{RecMuons} E_{x,y},$$

and again summing in quadrature. Finally, $E_T^{Miss,Cryo}$ term is calculated from reconstructed jet corrections terms

$$E_{x,y}^{Miss,Cryo} = -\sum_{RecJets} E\,jet_{x,y}^{cryo},$$

where $E\,jet_{x,y}^{cryo}$ is a calibrated correction term of the reconstructed jet energy in the third layer of the electromagnetic calorimeter and in the first layer of the hadronic calorimeter. This correction in energy is taken into account because the cryostat has a thickness of approximately half an interaction length which can absorb energy from a hadronic shower. The correction turns out to be non-negligible for high p_T jets; contributing 5% per jet with p_T over 500 GeV [10].

The object based reconstruction of E_T^{Miss} is carried out by analyzing low p_T deposits from such sources as neutral and charged pions, soft jets and pile-up and high p_T objects such as electrons, muons, taus and jets [10]. Again the algorithm makes use of topological clusters to group the cells, but it then distinguishes them into the two categories of either high or low p_T and the E_T^{Miss} is calculated by adding the contributions from each type [10]

$$E_{x,y}^{Miss,Final} = -E_{x,y}^{Miss,High} - E_{x,y}^{Miss,Low}.$$

While these E_T^{Miss} algorithms will eventually be indespensible in many beyond Standard Model searches, this study will not make use of these official algorithms, instead any E_T^{Miss} values used have been calculated from jet level quantities. The reason for this is that both algorithms rely on a detailed understanding of the topocluster objects, which in turn means they rely heavily on an understanding of the signal-to-noise ratio. The E_T^{Miss} alogorthims are themselves under detailed study.

3 Data and Run Information used in Analysis

In the analysis that follows, data have been utilizied from three different sources: JX QCD Jet Monte Carlo (MC) simulations, M7 cosmic ray run 69373, and cosmic ray Monte Carlo simulations.

3.1 JX QCD Jet Monte Carlo

The JX Jet MC is a Pythia generated simulation that utilizes the Lund string model of hadronization. This model of hadronization treats all but the highest p_T gluons as colour charged field lines, which are attracted to one another by the non-abelian gluon self interaction. The string fragmentation represents the parton fragmentation during a hard pp scatter [11].

The following JX samples have been utilized in this study [12]:

J2 (QCD JETS): ***trig0_calib0_csc11.005011.J2_pythia_jetjet.recon.NTUP.v12000701***
P_T of hard scatter from 35 to 70 GeV.
Cross Section: $9.33 \times 10^7 pb$.

J3 (QCD JETS): ***trig0_calib0_csc11.005012.J3_pythia_jetjet.recon.NTUP.v12000701***
P_T of hard scatter from 70 to 140 GeV.
Cross Section: $5.88 \times 10^6 pb$.

J4 (QCD JETS): ***trig0_calib0_csc11.005013.J4_pythia_jetjet.recon.NTUP.v12000701***
P_T of hard scatter from 140 to 280 GeV.
Cross Section: $1.08 \times 10^5 pb$.

J5 (QCD JETS): ***trig0_calib0_csc11.005014.J5_pythia_jetjet.recon.NTUP.v12000701***
P_T of hard scatter from 280 to 560 GeV.
Cross Section: $1.25 \times 10^4 pb$.

J6 (QCD JETS): ***trig0_calib0_csc11.005015.J6_pythia_jetjet.recon.NTUP.v12000701***
P_T of hard scatter from 560 to 1120 GeV.
Cross Section: $360 pb$.

3.2 M7 Cosmic Ray Run 69373

Run 69373 was a 13.69 hour cosmic ray run taken between 18:29:23 on 19 May 2008 and 8:11:53 on May 20, 2008 that recorded 104,646 events [13]. The full calorimetry system was the only detector sub-system taking data during this period. Both the Level-1 Calorimeter (L1Calo) and Random (RNDM0) triggers were in use, however, this study focuses on the L1Calo trigger.

The L1Calo trigger is a digital system designed to work with 7000 analogue trigger towers. The pre-processer digitizes the analog signals and uses a look-up table to produce the transverse energy values used in the trigger algorithms. These digitized data are then sent to the Cluster Processor (CP), which identifies electrons, photons, and taus, and the Jet Energy Sum Processor (JEP) which identifies "jet trigger elements" or 0.2×0.2 sums in $\Delta\eta \times \Delta\phi$. Within the CP and JEP data is compared to preset E_T thresholds [1]. The L1Calo triggers of interest used in this run are 1J4, and 1J5 jet triggers which trigger on regions of interest (RoI) in the calorimeters with greater than 4 GeV and 5 GeV of E_T respectively and the 1EM2 and 1EM3 electromagnetic triggers which trigger on RoI's with electromagnetic E_T greater than 2 GeV and 3 GeV respectively [13].

3.3 Cosmic Monte Carlo

The Cosmic Monte Carlo data set used in this study uses a simulation which generates muons at the surface above the ATLAS Cavern in numbers coinciding with measured cosmic ray flux [14]. The muons are then propagated through the ground, and access shafts, separating ATLAS

from the surface. The muons which survive the journey are then simulated interacting with the detector. However, since no trigger information is provided in this simulation, even minimum ionizing muons are recorded as interacting with the detector [14].

4 QCD Jets and Cosmics

The ability to distinguish between real QCD jets resulting from pp collisions and high energy cosmic ray muons, which have been reconstructed as jets, is going to be important to any physics analysis with E_T^{Miss} event topologies. By examining the p_T, E_T^{Miss}, and m_{eff} distributions, it is evident that periods of time on the scale of hours are enough to produce a few high energy events from cosmic rays. Running jet reconstruction algorithms on cosmic ray events also allows for the very first test of the algorithms on real data.

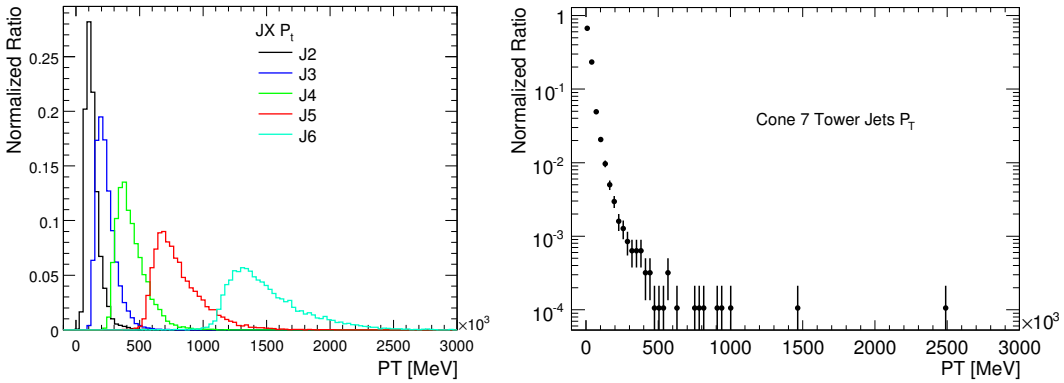

Figure 1: p_T distributions for both JX MC jet events, and cosmic ray events.

Figure 1 shows the p_T distributions for both JX jet events, and cosmic ray events. The distributions have been normalized to show percentage of events with a given p_T to allow easier comparsion between data sets with differing numbers of events. The distributions have been calculated by summing over the scalar transverse energy in all events to obtain a scalar p_T distribution within a factor of c. While the JX distribution simply re-iterates what is known about the particular J samples p_T binning, the cosmic distribution illustrates the large number of high p_T events that can be reconstructed as background once collisions begin. Thirteen cosmic events having $p_T > 500GeV$ have been reconstructed in this run.

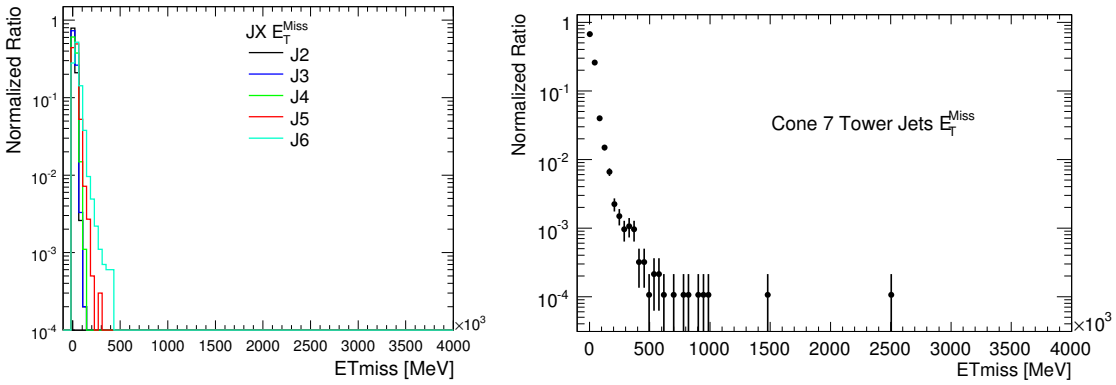

Figure 2: E_T^{Miss} distributions for both JX MC jet events, and cosmic ray events.

The E_T^{Miss} distributions in shown in Figure 2 have been calculated by summing the transverse momentum of the jets in x and y over all events and adding them in quadrature. As would be expected there is very little E_T^{Miss} in the JX samples, with no events exceeding 500 GeV. The cosmic ray distribution is nearly identical to the p_T distribution, which is also expected, since any energy deposit from a cosmic muon in the barrel calorimeters is going to be asymmetrical in ϕ. This asymmetry is caused by the cosmic muons depositing large amounts of energy within a very small number of cells in the calorimeter. Since the L1Calo triggers have thresholds on the order of a few GeV, no minimum ionizing particles are going to be detected and only muons which interact via a hard bremsstrahlung will be recorded.

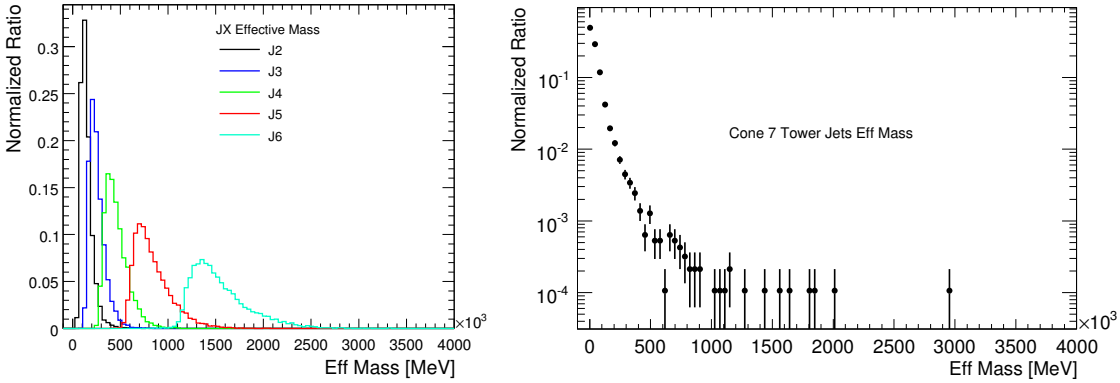

Figure 3: m_{eff} distributions for both JX MC jet events, and cosmic ray events.

Finally, in Figure 3, the m_{eff} is shown. The m_{eff} for these distributions was calculated by adding the E_T^{Miss} and the p_T together. Conventionally the m_{eff} would be calculated from the E_T^{Miss} and the p_T of the four hardest jets in each event, however, in these distributions all jets have been considered. The m_{eff} plot is important as a discovery plot for many new physics channels, particularly supersymmetry [15]. This is because the SUSY mass scale can be inferred by measuring the peak of the m_{eff} distribution, when Standard Model once Standard Model backgrounds have been removed.

5 Data Cleaning with F_{EM}

The electromagnetic fraction (F_{EM}) is a measure of how much energy is deposited into a calorimeter system's electromagnetic and hadronic components. It can be calculated at the calorimeter cell level, or with reconstructed objects such as jets. In this study the F_{EM} has been calculated for the JX sample MC, reconstructed cosmic ray jets, as well as cosmic ray MC. While the F_{EM} for JX samples and the cosmic ray events was calculated at the jet level, the F_{EM} of the cosmic ray MC was calculated at a cell level. The reason for the two different calculation methods is due to the fact that the commissioning combined Ntuple (CBNT) used for the cosmic MC data, lacked the necessary quantities to calculate the F_{EM} at the jet level.

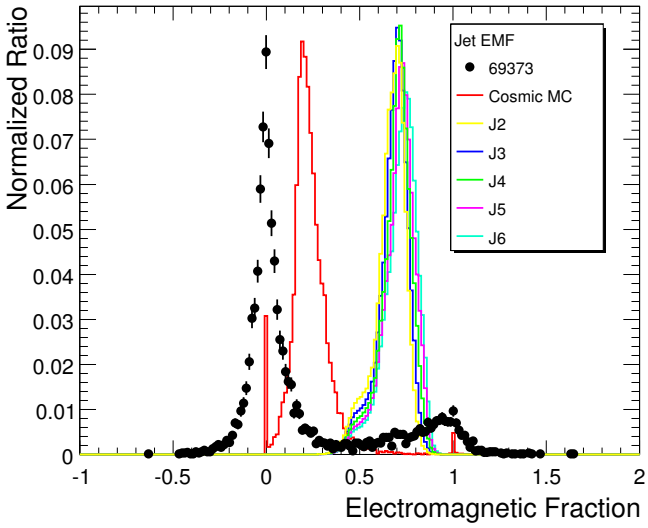

Figure 4: F_{EM} for JX samples, cosmic events, and cosmic MC.

The F_{EM} values displayed in Figure 4 have been calculated using two separate techniques. For the JX samples, and cosmic events it was calculated using the jet electromagnetic energy and the jet total energy:

$$F_{EM} = \frac{JetE_{EM}}{JetE_{Total}}.$$

While the cosmic MC quantity was calculated by summing all the cell energies in the electromagnetic and hadronic calorimeters, and looking at the total fraction:

$$F_{EM} = \frac{CellE_{EM}}{CellE_{EM}+CellE_{HAD}}.$$

The discrepancy between the cosmic ray data and cosmic MC is due primarily to lack of trigger information in the MC. Clearly, however, the F_{EM} is providing a robust way of distinguishing between genuine QCD jets and cosmic rays which have faked jets. The QCD jets show a distribution peaked around 0.7, while the cosmic jet distribution peaks around 0. This is explained by the fact that a QCD jet will deposit close to equal amounts of energy in both the electromagnetic and hadronic portions of the calorimeter, while a cosmic ray is more likely to deposit it's energy

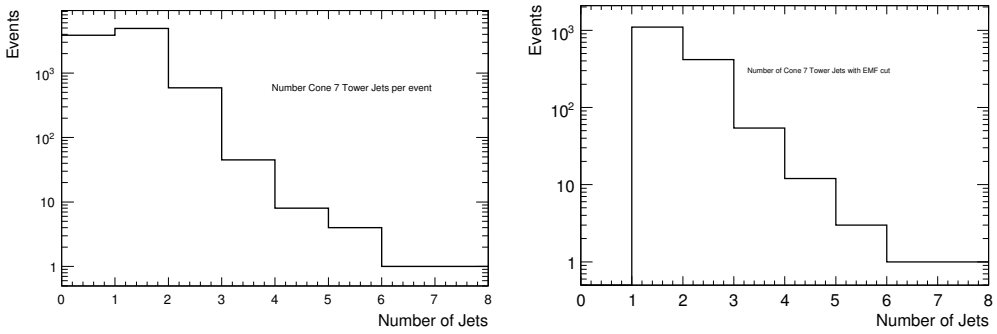

Figure 5: Number of reconstructed jets from cosmic rays, before and after an F_{EM} cut of 0.2.

within the much larger hadronic calorimeter, simply because it presents many more radiation lengths of material.
An F_{EM} cut of 0.2 reduces the total number of reconstructed jets from 5982 to 1981, a reduction of 67%. This reduction is even more evident within the E_T^{Miss}, and m_{eff} distributions.

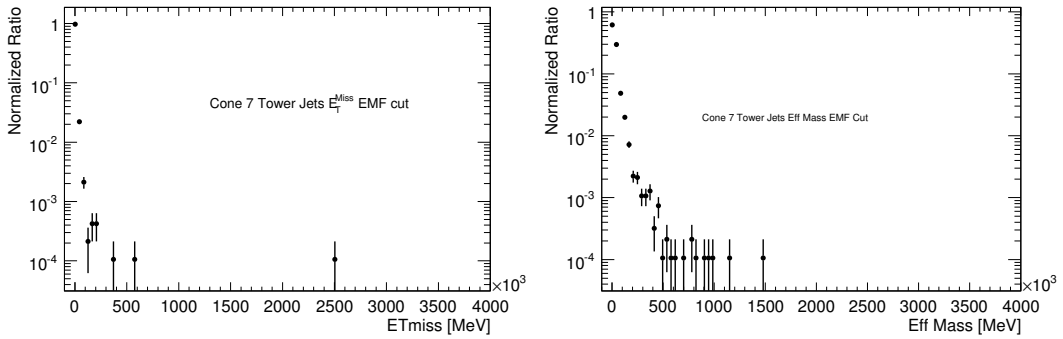

Figure 6: E_T^{Miss} and m_{eff} distributions of cosmic events, after and F_{EM} cut of 0.2.

After an F_{EM} cut of 0.2, the E_T^{Miss} distribution of cosmic rays has been significantly reduced,with number of events with $E_T^{Miss} > 300GeV$ down to 3 from 48, a reduction of 94%. To further investigate the three high E_T^{Miss} events that remain, the ATLANTIS event display [16] is used to view the pulse shapes coming out of the calorimeter cells.

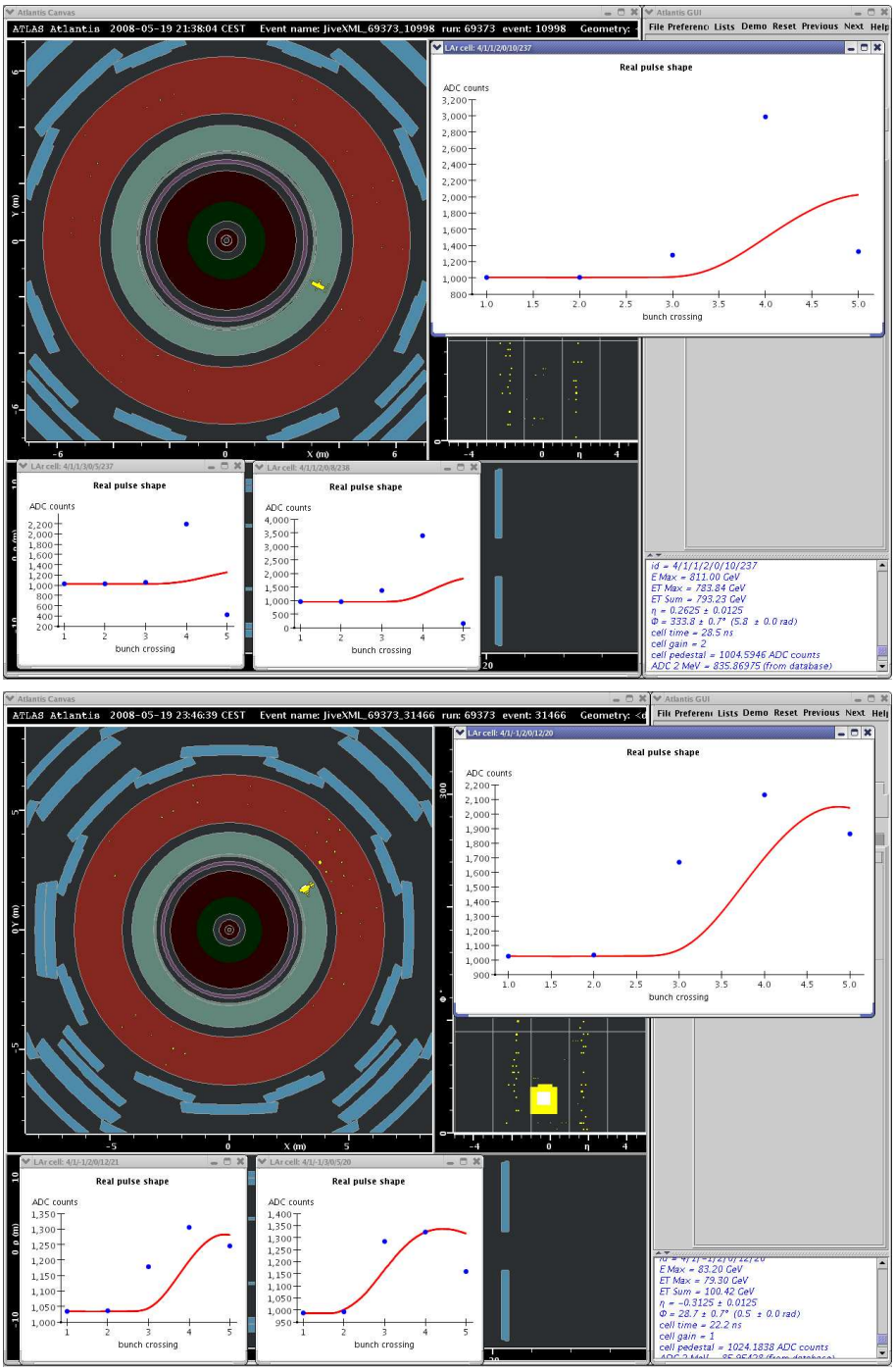

Figure 7: Atlantis event displays of LAr cells in events 10998 and 31466, from run 69373.

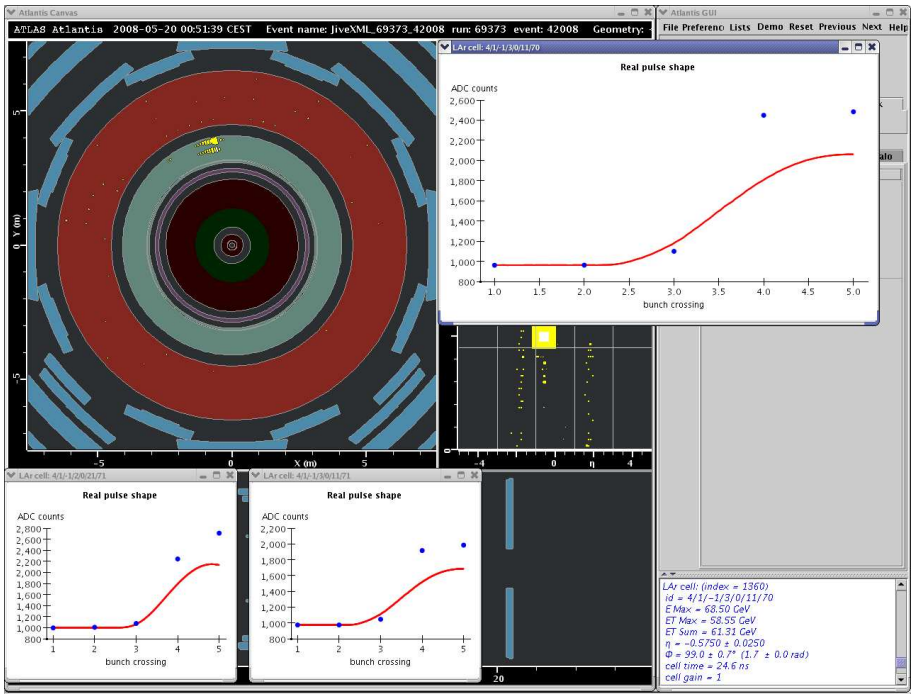

Figure 8: ATLANTIS event display of LAr cells in event 42008, from run 69373.

Figures 7 and 8 show event displays and pulse shapes for the three events with $E_T^{Miss} > 300GeV$ that survive the F_{EM} cut of 0.2. The pulse shapes shown in each case are for the highest energy LAr cell in the event (in upper right corner), as well as two surrounding LAr cells. All three events exhibit abnormal pulse shapes, in the high energy cells as well as the surrounding cells. The timing in each event appears to be shifted, as in ideal conditions the reconstructed pulse shape as well as the data would be centered around the third bunch crossing. Finally, the reconstructed pulse shapes are not fitting the data, which could indicate a problem with the reconstruction algorithm in the software. Events which do not survive the F_{EM} cut, do not exhibit such abnormal shapes.

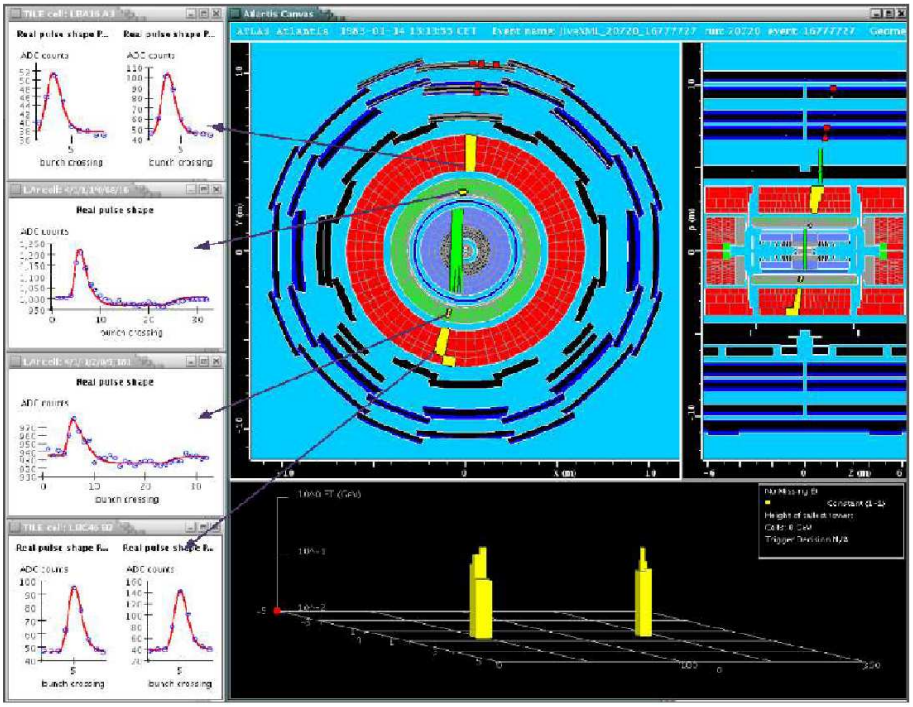

Figure 9: ATLANTIS event display from an M4 commissioning run showing what properly reconstructed LAr cell pulse shapes should look like.

Figure shows an event display from a cosmic event taken during milestone week 4 (M4), which shows what properly reconstructed LAr pulse shapes should look like. Unfortunately, since 69373 was a 5 sample run, and not a 32 sample debugging run, not much more can be said about these irregular pulse shapes.

Further analysis of calorimeter timing may be used to identify these high energy deposits as cosmic rays or simply noisy channels. The timing in the ATLAS calorimeters is such that particles arriving in the calorimeters have time $t = 0$. Cosmic ray events however, will not follow such a timing scheme, and one identification method is to calculate the "up-minus-down" time of the calorimeter, once it has been divided symmetrically in ϕ. A regular jet event should yield an "up-minus-down" peaking around zero, while a large energy deposit from a cosmic ray event will have an offset peak, due to the asymmetry in ϕ of its interaction with the calorimeter [17].

6 Conclusion and Future Work

The first part of this study has focused on the comparison of JX MC jet samples, and jets reconstructed from high energy cosmic ray events. This comparison is useful in that it allows for some of the very first analysis in ATLAS performed with real data instead of just simulations. Working all the way from data collection, through reconstruction, to data analysis on real events is crucial in giving the ATLAS detector, and software its first real "workout", leading up to the first collisions.

The second part focuses on using the jet electromagnetic fraction as a cleaning technique to remove sources of fake E_T^{Miss}. This method proves to be very robust in reducing the number of

jets reconstructed from high energy cosmic ray events, as well as removing them from the jet E_T^{Miss} distribution. High energy events that do survive an EMF cut are then examined using the ATLANTIS event display to check for irregularities in their cell read-out pulse shapes.

This study will be carried on with further cosmic ray data to examine more cleaning techniques, such as calorimeter timing [16], as well as to gain further understanding of jet and E_T^{Miss} reconstruction algorithms. Looking ahead to September, fully circulating beams in the LHC [2] will produce "beam-gas" events within ATLAS which will provide further data to analyze before actual collisions. Finally, once the LHC begins producing collisions within ATLAS, the knowledge gained through this study will provide an excellent starting point to begin analyzing jet and E_T^{Miss} events.

References

[1] ATLAS Collaboration, The ATLAS Experiment at the CERN Large Hadron Collider, JINST 3 S08003, (2008).

[2] LHC First Beam, 14 August 2008, web page: http://lhc-first-beam.web.cern.ch.

[3] R. Wigmans, Calorimetry: Energy Measurement in Particle Physics, (Oxford Science Publications, Oxford, 2000).

[4] ATLAS Collaboration, Jet Reconstruction Performance in the ATLAS Detector, (2008), http://cdsweb.cern.ch/record/1103728.

[5] ATLAS Detector Commissioning, 17 August 2008, web page: http://atlas-computing.web.cern.ch/atlas-computing/projects/commissioninglax .

[6] The Athena Framework, 18 August 2008, web page: http://twiki.cern.ch/twiki/bin/view/Atlas/AthenaFrameWork.

[7] ATLAS Computing Group, ATLAS Computing Technical Design Report, ATLAS TDR 017, CERN/LHCC/05-22, (2005).

[8] ATLAS Collaboration, ATLAS Performance and Physics Technical Design Report, ATLAS TDR 014, CERN/LHCC/99-15, (1999).

[9] P. Loch, Jets and ETmiss, Trigger and Offline Board Meeting, 21 May 2008, web page: http://indico.cern.ch/conferenceDisplay.py?confId=26481.

[10] ATLAS Collaboration, Measurement of Missing Transverse Energy in ATLAS, (2008), http://cdsweb.cern.ch/record/1103728.

[11] Pythia, 19 August 2008, web page: http://home.thep.lu.se/ torbjorn/pythia.html.

[12] Jet CSC Simulation Production, 16 August 2008, web page: https://twiki.cern.ch/twiki/bin/view/Atlas/JetCSCSimulation.

[13] ATLAS Run Summary Information, 16 August 2008, web page: http://atlas-service-runinformation.web.cern.ch/atlas-service-runinformation/.

[14] M. Boonekamp *et al*, Cosmic Ray Beam-Halo and Beam-Gas Rate Studies for ATLAS Commissioning, ATL–GEN-2004-001 (2008), http://documents.cern.ch/cgi-bin/setlink?base=atlnotcateg=Noteid=gen-2004-001.

[15] S. Asai, Plots of 1 TeV SUSY, SUSY Working Group General Meeting, 29 August 2007, web page: http://indico.cern.ch/conferenceDisplay.py?confId=18251.

[16] Atlantis Event Display, web page: http://cern.ch/atlantis/.

[17] R.J. Teuscher *et al*, Fake Missing Transverse Energy from ATLAS Calorimeter Cosmic Ray Data, ATL–COM-CAL-2008-002 (2008), http://cdsweb.cern.ch/record-restricted/1087919.